VISCOPLASTICITY BASED ON OVERSTRESS WITH A DIFFERENTIAL GROWTH LAW FOR THE EQUILIBRIUM STRESS

E. Krempl, J.J. McMahon[1], D. Yao
Department of Mechanical Engineering
Aeronautical Engineering & Mechanics
Rensselaer Polytechnic Institute
Troy, New York 12181

Two coupled, nonlinear differential equations are proposed for the modeling of the elastic and rate (time)-dependent inelastic behavior of structural metals in the absence of recovery and aging. The structure of the model is close to the unified theories but contains essential differences. The properties of the model are delineated by analytical means and numerical experiments.

It is shown that the model reproduces almost elastic regions upon initial loading and in the unloading regions of the hysteresis loop. Under loading, unloading and reloading in strain control the model simulated the experimentally observed sharp transition from nearly elastic to inelastic behavior. These properties are essential for modeling mean stress effects in tension-tension strain cycling. When a formulation akin to existing unified theories is adopted the almost elastic regions reduce to points and the transition upon reloading is very gradual.

For different formulations the behavior under sudden in(de)creases of the strain rate by two orders of magnitude is simulated by numerical experiments and differences are noted.

The model presently represents cyclically neutral behavior and contains three constants and two positive, decreasing functions. It is described how these constants and functions can be determined from tests involving monotonic loading with strain rate changes and relaxation periods.

---

[1] Now at NASA, Houston, Texas.

INTRODUCTION

Within the last decade the modeling of inelastic deformation through unified constitutive equations has made considerable progress [1-6]. With the exception of [5], yield surfaces are not used in these approaches and creep and time independent plasticity are not considered separately. It is shown in [6] that these constitutive equations have similar mathematical structure but that they differ with regard to the specific choices of material functions.

The models make the inelastic strain rate a function of the effective stress defined as stress minus some quantity referred to as kinematic stress, rest stress or back stress. In examining the mathematical properties of a first-order nonlinear differential constitutive equation it was shown [7] that making the inelastic strain rate solely dependent on the overstress gives qualitative solution properties of the differential equations found in corresponding experiments. The overstress is the difference between the stress and the equilibrium stress and is equivalent to the effective stress mentioned above.

This approach has been verified for monotonic loading of Type 304 SS [8] and of a Ti alloy [9]. The purpose of the present paper is to present a further development of the theory of viscoplasticity based on overstress for cyclic loading. It will be shown that this development is similar to the unified theories but contains essential modifications which are necessary for reproducing regions of nearly elastic behavior and realistic reloading behavior. These properties are basic for the modeling of mean stress effects in zero to maximum strain strain controlled cycling.

THE MAIN PROPOSED MODEL

Differential Formulation

For the uniaxial state of stress with σ and ϵ denoting the engineering stress and infinitesimal strain, respectively, the model is given by the two coupled nonlinear differential equations

$$\dot{\epsilon} = \dot{\epsilon}^{e\ell} + \dot{\epsilon}^{in} = \dot{\sigma}/E + \frac{\sigma - g}{Ek[\sigma - g]} \tag{1}$$

$$\dot{g} = \psi[\ ]\dot{\epsilon} - \frac{g - f[\ ]}{b[\ ]}\,|\dot{\epsilon}^{in}| \ . \tag{2}$$

In the above E is the elastic modulus and square brackets following a symbol denote "function of." The positive, bounded, decreasing function k is called the viscosity function, it has the dimension of time and controls the rate dependence. In the growth law for the equilibrium stress g there are three positive bounded functions, ψ, f and b, the argument of which will be determined in the sequel. For this

reason their arguments are not specified presently. A superposed dot denotes differentiation with respect to time and the absolute value of a quantity is denoted by placing it between vertical bars.

At the present this constitutive equation does not have any provisions for modeling recovery and/or aging. It is therefore only applicable in regions where these two phenomena are not pronounced.

By using the chain rule (1) and (2) can be rewritten as

$$\frac{d\sigma}{d\epsilon} = E - \frac{\sigma - g}{k[\sigma - g]\dot{\epsilon}} \tag{3}$$

$$\frac{dg}{d\epsilon} = \psi - \frac{g - f}{b}\left|1 - \frac{1}{E}\frac{d\sigma}{d\epsilon}\right| \operatorname{sign} \dot{\epsilon} \ . \tag{4}$$

The basic equations (1) - (4) will now be reformulated so as to identify the as yet unspecified functions with physical properties and to obtain mathematical properties of this system of nonlinear differential equations.

Integral Formulation

Following the procedures of [7], (1) and (2) can be transformed to the integral relations

$$\sigma - g = (\sigma_o - g_o)\exp - \int_{t_o}^{t} \frac{d\tau}{k} + \int_{t_o}^{t} (E\dot{\epsilon} - \dot{g})\left(\exp - \int_{\tau}^{t} \frac{ds}{k}\right)d\tau \tag{5}$$

and

$$g - f = (g_o - f_o)\exp - \int_{t_o}^{t} \frac{|\dot{\epsilon}_{in}|}{b}\,d\tau + \int_{t_o}^{t} (\psi\dot{\epsilon} - \dot{f})\left(\exp - \int_{\tau}^{t} \frac{|\dot{\epsilon}_{in}|}{b}\,ds\right)d\tau \tag{6}$$

respectively. A subscript zero indicates the value of the subscripted quantity at the initial time $t = t_o$.

Since the integrand of each first term on the right-hand side of (5) and (6) is positive its value will tend to zero for large times, provided that in (6) $|\dot{\epsilon}^{in}|$ will be different from zero as time increases.

The second terms tend to a limiting value for infinite time [7] so that

$$\{\sigma - g\} = \left\{E - \frac{dg}{d\epsilon}\right\} \dot{\epsilon} k\left[\{\sigma - g\}\right] \tag{7}$$

and

$$\{g - f\} = \left\{\psi - \frac{df}{d\epsilon}\right\} \left\{\frac{b}{|\dot{\epsilon}^{in}|}\right\} \dot{\epsilon} \tag{8}$$

where braces denote asymptotic values. By differentiation of (5) and (6) and taking the limit for $t \to \infty$ [7]

$$\{\dot{\sigma}\} = \{\dot{g}\} \tag{9}$$

and

$$\{\dot{g}\} = \{\dot{f}\} \tag{10}$$

are, respectively, obtained.

It is evident that (1) and (2) require σ, g and f to grow ultimately at the same rate, provided the functions have the properties stated initially and that $|\dot{\varepsilon}^{in}|$ does not become zero for large times. Also from (7) and (8) it is required that $\dot{\varepsilon}$ be bounded and constant for large times.

Behavior Under Instantaneous Changes in Stress or Strain Rate

The behavior of (1) under an instantaneous change in stress or strain rate has been determined in [10-12].

A superposed +(-) designates the value of a quantity immediately after (before) the jump. Then applying (3) and (4) before and after the jump yields ($\dot{\varepsilon}^{in}$ is continuous under a jump)

$$\left(\frac{d\sigma^+}{d\varepsilon} - E\right)\dot{\varepsilon}^+ = \left(\frac{d\sigma^-}{d\varepsilon} - E\right)\dot{\varepsilon}^- \tag{11}$$

and

$$\frac{dg^+}{d\varepsilon} = \frac{dg^-}{d\varepsilon}\frac{\dot{\varepsilon}^-}{\dot{\varepsilon}^+} + \psi\left(1 - \frac{\dot{\varepsilon}^-}{\dot{\varepsilon}^+}\right) \quad \text{for strain control} \tag{12a}$$

$$\frac{dg^+}{d\varepsilon} = \frac{dg^-}{d\varepsilon}\frac{\dot{\sigma}^-}{\dot{\sigma}^+}\alpha + \psi\left(1 - \alpha\frac{\dot{\sigma}^-}{\dot{\sigma}^+}\right) \quad \text{for stress control} \tag{12b}$$

where $\alpha = \dfrac{d\sigma^+/d\varepsilon}{d\sigma^-/d\varepsilon}$. It is seen that the slope of g is related to that of σ but the slope of σ is not influenced by g at all. As a consequence the properties of $d\sigma/d\varepsilon$ as determined in [10-12] remain unaltered.

If it is now assumed that the asymptotic properties (7) - (10) and $d\sigma^-/d\varepsilon \approx E_t \ll E$ with $E_t \geq 0$ the tangent modulus[1] in the inelastic range hold, then the slopes of σ and g can be calculated for increase, decrease, reversal, reversal with increase and reversal with decrease of the stress or strain rate. Under the above assumptions (12) simplifies to

---

[1] This designates the slope at the limit of the region of interest.

$$\frac{dg^+}{d\epsilon} = \psi + \frac{\dot{\epsilon}^-}{\dot{\epsilon}^+}(E_t - \psi) \quad \text{for strain control} \tag{13a}$$

and

$$\frac{dg^+}{d\epsilon} = \psi + \frac{\dot{\sigma}^-}{\dot{\sigma}^+}(E_t - \psi)\,\frac{d\sigma^+/d\epsilon}{E_t} \quad \text{for stress control} \tag{13b}$$

It can be observed that no changes in the slope of g are realized when the asymptotic value of ψ is equal to E_t.

Values obtained from (11) and (13a), (13b) are given in Table 1 where it is assumed that rate changes involve at least one order of magnitude.

Creep and Relaxation Behavior

During relaxation $\dot{\epsilon} = 0$ and from (1) and (2)

$$\dot{\sigma} = -\frac{\sigma - g}{k[\sigma - g]} \tag{14}$$

and

$$\dot{g} = -\frac{g - f}{b}\,|\dot{\epsilon}^{in}| \tag{15}$$

respectively. It is seen that both $\dot{\sigma} < 0$ and $\dot{g} < 0$, if $\sigma - g > 0$ and $g - f > 0$. From (5) and (6) it can be deduced that these conditions are met at any point during a prior tensile test provided $\dot{\epsilon} > 0$ and $E - \frac{dg}{d\epsilon} > 0$ and $\psi - \frac{df}{d\epsilon} > 0$. (If $\dot{\epsilon} < 0$ the sign of $\sigma - g$ and $g - f$ reverses and $\dot{\sigma}$ and $\dot{g}$ are positive.) Therefore σ and g always decrease in magnitude but not uniformly. Indeed from (14) and (15)

$$\frac{\dot{\sigma}}{\dot{g}} = \frac{bE}{g - f} \tag{16}$$

Unless $(g - f)/b < E$ the quantity on the right-hand side exceeds one and $\dot{\sigma} > \dot{g}$, so that σ relaxes faster than g.

Stress relaxation stops at $\sigma = g$ but since $\dot{g}$ is zero at both $\sigma = g$ and at $g - f$ it is not clear whether equilibrium is reached at $g = f$, or at $g > f$ when $\sigma = g$. If the right-hand side of (16) is greater than one it is expected that $\dot{\sigma} = 0$ at $g > f$.

In creep (1) and (2) specialize to (σ_c is the constant stress in the creep test)

$$\dot{\epsilon} = \frac{\sigma_o - g}{Ek[\sigma_o - g]} \tag{17}$$

and

$$\dot{g} = \psi\dot{\epsilon} - \frac{g - f}{b} |\dot{\epsilon}| , \qquad (18)$$

respectively. It is seen by comparing (18) and (2) that the growth of g in creep is slightly modified compared to constant strain rate loading since in creep $\dot{\epsilon} = \dot{\epsilon}^{in}$. Differentiation of (17) yields

$$\ddot{\epsilon} = - \frac{\dot{g}}{k^2 E} (k - (\sigma_o - g)k') \qquad (19)$$

where $k' = \frac{dk[x]}{dx} < 0$ by initial stipulation. Secondary creep will be obtained when $\dot{g} = 0$ and this is accomplished when $\dot{f} = \frac{df}{d\epsilon} \dot{\epsilon} = 0$, i.e., when the tangent of f is ultimately horizontal, see (10). Primary creep results if $\dot{g} > 0$. In this case creep terminates at $\sigma_o = g$. If $\sigma_o > g$ for all values of g creep will never terminate.

REQUIREMENTS ON A REALISTIC MODEL

The following requirements are put on the model:

1) There is an initial nearly linear elastic region starting from zero to some finite stress. In this region there is not only $d\sigma/d\epsilon = E$ but there is also no creep and relaxation.

2) After unloading there is again an elastic region with the same properties as 1) which starts below the stress at which reversal begins and can end at zero stress but usually ends at a stress magnitude larger than zero.

3) When a creep test is performed at zero stress after prior inelastic deformation the strain magnitude will either stay constant or will decrease. However, equilibrium will be reached very close to the inelastic strain at which the creep test started. In no way should the strain magnitude increase nor should zero strain be reached at equilibrium if the strain magnitude decreases. (Aftereffect, recovery test.)

4) After the initial linear elastic region inelastic deformation sets in characterized by a tangent modulus much less than the elastic modulus. The material exhibits normal rate sensitivity (an increase in rate increases the stress level), creep and relaxation. (The region of creep and relaxation may already begin upon loading before $d\sigma/d\epsilon$ decreases appreciably.)

5) Primary and secondary creep may be experienced together with possible "anomolous" creep behavior. (Creep rate may not necessarily increase with stress increase, at the same stress level creep rate is higher on loading than on unloading, see [6,8,13,14].)

6) When relaxation behavior is considered it is not uniform everywhere on the hysteresis loop. It is most pronounced where the tangent modulus is low. It is minimal when the tangent modulus is close to the elastic modulus below the stress at which unloading started and above zero stress. At zero stress relaxation, if it occurs, is small and such that the stress magnitude increases [14,15]; see also 2).

7) After unloading to zero stress and subsequent reloading in strain control the transition to inelastic deformation is very sharp. A small hysteresis loop may develop in the quasielastic region.

8) In cyclic loading cyclic hardening, softening or cyclic neutral behavior should be reproduced.

9) The behaviors listed in 3) - 8) should not be peculiar to a certain stress or strain value or region. Rather they are inelastic properties found in the nonelastic regions.

SELECTION OF FUNCTIONS ψ, f AND b

In the following the simplest choice for these functions will be made such that the requirements listed above will be met as far as possible. The choices have been arrived at after numerous numerical experiments [16,17] which included other possibilities than those allowed by (1) and (2).

In view of (9) and (10)

$$f = E_t e \ . \tag{20}$$

This selection permits the final slope of the stress-strain diagram to be selected by the usual choice $E_t \geq 0$. (The model permits the use of a negative E_t. This will be explored in the future.)

The choice

$$\psi = \psi[\sigma - g] > 0 \tag{21}$$

with

$$\psi' < 0 \ , \ \psi[0] = \bar{E} < E$$

and $\psi[-x] = \psi[x]$ helps to satisfy conditions 1) - 3), 6), 7) and 9). (It is not possible to have ψ depend on $\sigma - g$ and to have $\psi[0] = E$. In this case (1) and (2) produce only linear elastic behavior. For this reason $\bar{E} = 0.99\ E$ is usually chosen.)

This choice makes g rate dependent, see (8). In this case k and g would both be responsible for rate dependence and inverse rate-sensitivity could be modeled (the stress decreases upon an increase in stress (strain) rate). However, for the present purposes it was decided to make the

asymptotic value of g - f and therefore of g independent of rate by selecting

$$b = \frac{A}{\psi[\sigma - g] - E_t} \tag{22}$$

where $A > 0$ is the asymptotic value of $\{g - f\}$. With this choice g will be rate dependent after the initial elastic region and before the asymptotic solution is reached. However, the initial and final properties of g are independent of loading rates.

Using (22), (1) and (2) reduce to

$$\dot{\epsilon} = \frac{\dot{\sigma}}{E} + \frac{\sigma - g}{Ek[\sigma - g]} \tag{23}$$

$$\dot{g} = \psi[\sigma - g]\dot{\epsilon} - \frac{(g - E_t\epsilon)(\psi[\sigma - g] - E_t)}{A} |\dot{\epsilon}^{in}| \ . \tag{24}$$

In this version the model has two free functions k and ψ and three positive constants with dimensions of stress E, E_t and A which permit fitting to experimental data of a given material. The functions k (dimension time) and ψ (dimension stress) are restricted to be positive and to decrease with increasing argument. Appropriate mathematical forms must be found and their choice will influence rate dependence (k) and the shape of the stress-strain diagram especially the transition from elastic behavior to inelastic behavior (ψ). A procedure for curve fitting is given in the Appendix.

With this choice of functions the model represents symmetry with regard to the origin and a generalized Masing hypothesis. To illustrate this consider a test starting from the origin loaded with constant $\dot{\epsilon}$ in compression. Another test is first loaded to some positive value of stress and strain, so that $\sigma_o - g_o > 0$ and $g_o - f_o > 0$, before loading with the same $\dot{\epsilon}$ in compression as the first test. From (5) and (6) we see that <u>ultimately</u> both tests produce the same g - f and σ - g. Since $f = E_t\epsilon$ the same g and therefore the same σ will be finally obtained, see also (7) and (8).

Because of these properties the model does not reproduce cyclic hardening or softening. These properties require that one or more constants be made dependent on an accumulating measure of history such as the inelastic strain path length. Another possibility is to postulate an extra growth law for A which controls the stress level and/or to make E_t depend on, say, the inelastic strain-path length. These additions are under development.

Whether or not these ultimate values are obtained at strain levels of interest depends on how fast the first terms on the right-hand side of (5) and (6) become negligible. Experience with numerical experiments

has shown that these asymptotic values can be obtained with reasonable accuracy at strains of one percent.

Aside from these general properties the details must be evaluated through numerical experiments, i.e., the automatic integration of (23) and (24) subject to various stress or strain histories. This will be done presently by selecting the constants and functions. Numerical integration was performed using the IMSL program DGEAR on an IBM 3033 or 3081D computer.

DISCUSSION AND NUMERICAL EXPERIMENTS

Relation to Other Models

The present model falls in the general category of the unified models which do not separately consider the actions of creep and plasticity. According to [6] the unified models can be written as

$$\dot{\varepsilon} = \dot{\varepsilon}^{el} + \dot{\varepsilon}^{in} \tag{25}$$

$$\dot{\varepsilon}^{in} = F\left[\frac{\sigma - \Omega}{K}\right]; \quad F[0] = 0; \quad F[-x] = -F[x] \tag{26}$$

$$\dot{\Omega} = f_1 \dot{\varepsilon}^{in} - f_2 \Omega |\dot{\varepsilon}^{in}| - f_3 |\Omega| \tag{27}$$

$$\dot{K} = f_4 \dot{\varepsilon}^{in} - f_5 K |\dot{\varepsilon}^{in}| - f_6 K \tag{28}$$

where $f_1 - f_6$ are either positive constants or positive functions of one, two or three of the variables σ, Ω and K.

Comparison of (23) through (28) with (1) and (2) reveals the following:

i) The functions f_3 and f_6 are absent

ii) The variable K is not represented

iii) ψ assumes the role of f_1 but it is multiplied by $\dot{\varepsilon}$ instead of $\dot{\varepsilon}^{in}$.

The reasons for these choices are:

i) Since the model is intended for regions where recovery of hardening (annealing) are considered to be insignificant the recovery terms f_3 and f_6 are omitted.

ii) The isotropic drag stress term is not included since it implies that rate sensitivity changes significantly with deformation behavior. Inversion of (26) yields

$$\sigma - \Omega = KF^{-1}(\dot{\varepsilon}^{in}) . \tag{29}$$

It demonstrates that the overstress (effective stress) $\sigma - \Omega$ is proportional to K. Comparing two specimens at the same inelastic strain rate, but different histories leading to different values of K would also lead to different effective stresses (overstresses) and therefore different rate sensitivities.

Elevated temperature experiments aimed at determining whether hardening is due to growth in Ω or to a growth in K or both are not known to the authors. Indeed a recent review does not address this question [18]. However, in [30] a change in K was inferred from a change in the stress drop with cycling during constant strain hold-time tests on 316 stainless steel at 600°C. Experiments at room temperature on the strongly hardening annealed Type 304 SS [19,20] showed that essentially all hardening was due to an increase in Ω. For cyclically neutral Ti-alloy no changes in Ω and K due to prior deformation were found [21].

Judging from a review of elevated temperature data [22,23] one might infer hardening primarily due to changes in Ω but this is not clear.

Because of these uncertainties it was decided to stay with the cyclically neutral model, see (23), (24). Moreover, even the room temperature experiments have shown results [20,21] which demonstrate that strong cyclic hardening cannot be adequately modeled with the present approaches, see also [24].

iii) The use of $\dot{\epsilon}$ instead of $\dot{\epsilon}^{in}$ to multiply the initial term in (24) will be disturbing to materials scientists who will argue that g is a state variable which should grow only when inelastic deformation occurs. Therefore the approach presented in (24) is not "physical." From (25), (26) and (27), and the chain rule

$$\left.\begin{aligned} \frac{d\sigma}{d\epsilon} &= E \\ \text{and} \qquad \frac{d\Omega}{d\epsilon} &= 0 \end{aligned}\right\} \tag{30}$$

are obtained, respectively, at the origin ($\sigma = 0$; $\Omega = 0$). On the other hand from (23) and (24)

$$\left.\begin{aligned} \frac{d\sigma}{d\epsilon} &= E \\ \text{and} \qquad \frac{dg}{d\epsilon} &= \psi[0] \ , \end{aligned}\right\} \tag{31}$$

so that the slope of g at the origin can be controlled by ψ. By a proper choice of $\psi[0]$ nearly linear elastic regions can be reproduced.

The difference between the two approaches is demonstrated in Figures 1 and 2. In both figures the evolution of σ and g under a strain controlled loading, unloading and reloading experiment are plotted. The material functions used are listed in Table 2 (they

are not intended to represent a specific alloy and the difference between Figure 1 and Figure 2 is only that $\dot{\varepsilon}^{in}$ is used to multiply ψ in (2) or (24) in the former whereas $\dot{\varepsilon}$ is employed in the latter.

Regarding the evolution of σ both figures show the same initial slope. From then on the σ curve in Figure 1 is more gradual than in Figure 2. Upon reloading a sizeable hysteresis loop develops and the transition is gradual in Figure 1 whereas almost no hysteresis and a very sharp transition is observed in Figure 2. This sharp transition corresponds to that observed in strain controlled experiments [25].

Figure 1 also demonstrates the zero slope of the g (back stress) curve at the origin. Since the inelastic strain rate depends on $(\sigma - g)$ and since in strain control the same time is represented by the same strain it can be seen that only the origin and two other points in Figure 1 where σ and g intersect have zero inelastic strain rate. Elasticity is reduced to three isolated points in Figure 1. In all other regions creep and relaxation can be found. This fact is of course not noticeable if the figure does not contain the evolution of g.

In contrast, in Figure 2 there are regions where σ and g essentially overlap. In these regions nearly linear elastic behavior without noticeable creep and relaxation is reproduced.

This behavior is closer to reality than the one depicted in Figure 1 and partly for this reason we have chosen to use $\dot{\varepsilon}$ instead of $\dot{\varepsilon}^{in}$ in the growth law for g.

Aside from the existence of elastic regions the use of $\dot{\varepsilon}$ instead of $\dot{\varepsilon}^{in}$ makes quite a difference in the evolution of mean stress with cycles in a strain controlled test with positive mean strain. Figures 3 and 4 again depict results of numerical experiments under such loading. The only difference in the two graphs is the use $\dot{\varepsilon}^{in}$ in Figure 3 and of $\dot{\varepsilon}$ in Figure 4.

Qualitatively the results on Figure 4 are more realistic than those in Figure 3, see [12]. Because of this behavior the formulation with $\dot{\varepsilon}$ is preferred.

Figure 5 shows the results of numerical simulations such as depicted in Figures 3 and 4 for two strain ranges and two strain rates. The decay of mean stress is plotted vs cycles. It is evident that at the slow strain rate the decay is less rapid for the $\dot{\varepsilon}$ than for the $\dot{\varepsilon}^{in}$ formulation. However, when a fast strain rate (10^{-2} s^{-1}) is used the difference is less pronounced and the $\dot{\varepsilon}$ formulation predicts the smaller mean stress of the two.

The cycles depicted in Figures 3 and 4 occur in turbine disks and buckets. For their life prediction the remaining mean stress must be known from analysis. Figure 5 clearly demonstrates that the two formulations predict considerably different mean stresses.

The Material Functions of the Theory

In the absence of recovery and of cyclic hardening the present model has three constants and two material functions that must be identified. The method of identification which requires considerable expertise and uses the asymptotic solution properties (7) - (10) is described in the Appendix.

In contrast to other approaches [1-6] the specific forms of the functions are not given rather general properties are stated, see (21). Within these properties specific functions must be found to suit the specific application. It was demonstrated in [8,26] how k affects rate sensitivity and a selection of specific k-functions was given in [8].

The function ψ affects the knee of the stress strain diagram and the behavior upon rate changes, see Table 1. For the purposes of demonstrating its influence two forms of ψ are given in Table 2. One leads to an almost elastic viscoplastic behavior, see Figure 6, the other to a gradual transition from elastic to inelastic deformation, Figure 7.

Corresponding hysteresis loops are shown in Figures 8 and 9. It is seen that Masing behavior is represented in either case and that cyclic hardening is absent. The regions of nearly elastic behavior are clearly identified as those where σ and g coincide.

Note that the constants of the functions given in Table 2 are selected to give the same E_t and the same stress level, only the transition behavior is different.

Once the material functions have been set the behavior of the model is completely determined. As an example, the behavior at different strain rates and under strain rate changes shown in Figures 6 and 7 is cited.

Both figures show an effect of loading rate on g in the transition region which disappears after some strain has accumulated. The influence of rate on g is smaller but seems to disappear slower in Figure 6 than in Figure 7.

The transition from elastic to viscoplastic behavior for σ is sharp in Figure 6 but gradual in Figure 7. As the strain rate increases the sharpness of transition increases.

At point A in Figures 6 and 7 the strain rate is increased (reduced) by two orders of magnitude. Whereas little overshoot (undershoot) is observed in Figure 6 it is considerable for both the σ and g curves in Figure 7. After some transient period the original curves are traced over again. Again the transition period is longer in Figure 6 than in Figure 7.

The difference in behavior is solely attributable to the change in the function ψ. The question arises whether these overshoots could lead to instabilities. A separate stability analysis [27] shows that the critical points which are the asymptotic values of (23), (24) are stable. Even if there are overshoots (undershoots), they will be transient in nature, see also (5), (6).

Although overshoots (undershoots) are experienced in testing, see Figure 9 of [19], and [28], and are similar to those shown in Figure 7 the size of these transients is somewhat large.

If ψ in (24) is multiplied by $\dot{\varepsilon}^{in}$ a simple analysis corresponding to (12) and (13) shows that

$$\frac{dg^+}{d\varepsilon} = \frac{dg^-}{d\varepsilon}\frac{\dot{\varepsilon}^-}{\dot{\varepsilon}^+} = E_t\frac{\dot{\varepsilon}^-}{\dot{\varepsilon}^+} \tag{32}$$

and

$$\frac{dg^+}{d\varepsilon} = \frac{dg^-}{d\varepsilon}\alpha\frac{\dot{\sigma}^-}{\dot{\sigma}^+} = \frac{d\sigma^+}{d\varepsilon}\frac{\dot{\sigma}^-}{\dot{\sigma}^+} \tag{33}$$

for strain and stress control, respectively. It is clear that (32) and (33) lead to less variations of $dg^+/d\varepsilon$ than experienced with the $\psi\dot{\varepsilon}$ formulation, see Table 1. This is demonstrated in Figure 10 where the conditions are identical to those used in Figure 7, except for the multiplication of ψ by $\dot{\varepsilon}^{in}$. Very little overshoot is observed in this case.

The second term in (2) or (24) is multiplied by $|\dot{\varepsilon}^{in}|$ and has so far not been varied. If this term is replaced by $|\dot{\varepsilon}|$ the reloading behavior is similar to that shown in Figure 1. (See also [16], Figures 5.21 and 5.22.) It can be seen from (4) that $\frac{dg}{d\varepsilon} \approx \psi$ as long as $\frac{d\sigma}{d\varepsilon} \approx E$. Since under this condition $\sigma - g \approx 0$ and since $\psi[0] \approx E$ the slope of g remains very close to E as long as $\frac{d\sigma}{d\varepsilon} = E$ and the behavior results in the sharp transition upon reloading shown in Figure 2. If $|\dot{\varepsilon}^{in}|$ is replaced by $|\dot{\varepsilon}|$ in (2), (4) shows that the second term on the right-hand side is not negligible from the beginning and $\frac{dg}{d\varepsilon}$ decreases faster than in the previous case. (See [16] for a further discussion of the subject.)

A comparison of the hysteresis loops in Figures 8, 9 and 11 shows clearly the linear elastic regions for the $\psi\dot{\varepsilon}$-formulation which are absent in Figure 11. (Elastic regions are those where $\sigma = g$.) It is not possible to model regions of no creep and no relaxation in Figure 11 but Figures 8 and 9 display such regions.

CONCLUSIONS

Mathematical methods permit the establishment of some properties of the proposed constitutive equation, but numerical experiments are very necessary to investigate the detailed properties.

The proposed system which uses total strain rate in the growth law for the equilibrium stress (or back stress or kinematic stress) is able to reproduce regions of almost linear elastic behavior. If inelastic strain rate is used instead, these regions were shown to be absent.

Loading, unloading and reloading under strain control are reproduced in a realistic manner using the present approach. A much too gradual transition is exhibited when inelastic strain rate is employed instead.

These properties have an influence on the decay of mean stress under tension-tension strain controlled cycling. It appears that the present approach represents a realistic decay of mean stress. This quantity is important for fatigue life prediction of turbine components.

All comparisons were made by changing one parameter at a time. Although it is strongly suggested that presently available state variable theories share the qualitative properties of the present model with using the inelastic strain rate instead of the total strain rate a proof is outstanding. Such a proof requires numerical integration of the respective theories under the loading histories used in this paper.

ACKNOWLEDGEMENT

The financial support of NASA-Lewis Research Center and of the National Science Foundation made this research possible. Early on Dr. E.P. Cernocky suggested the structure for the growth law of the equilibrium stress.

APPENDIX

Determination of Material Functions

The model is given by (23) and (24) and contains three material constants (E, E_t, A)* and two material functions (k, ψ). Both functions must be continuous positive and decreasing functions. They are otherwise not specified. In applications specific forms must be chosen.

The elastic modulus E and the tangent modulus E_t are easily identified as the slopes of the stress-strain diagram at the origin and at the maximum strain of interest, respectively.

In determining k, ψ and A the asymptotic solutions (7) - (10) are needed and used. Points of g and the viscosity function k are determined as shown in [8] or [26]. The strain rate change tests proposed in [8] are preferred. The relaxation tests [26] are also useful provided the solution properties of (14) and (15) are accounted for (in [26] $g = g[\epsilon]$ only). Candidate functions for k are also given in [8, 26] but new ones may be easily proposed. In this step extrapolation, trial and error with judgement are required.

Once a point of g is known, the asymptotic value of $\{g - f\} = A$ can be determined from the corresponding value of σ and $f = E_t \epsilon$.

With $\psi[0] = \frac{dg}{d\epsilon}[0] = \bar{E}$, $\frac{dg}{d\epsilon}[\epsilon_{max}] = E_t$ and at least one point of g known, g can be approximated by the functions provided in [29] or by other representations (i.e., Ramberg Osgood relation). A similar procedure is used to approximate the stress-strain diagram. These two functions are now used as inputs to

$$\frac{dg}{d\epsilon} = \psi[\sigma - g;\ B, C, D] - \frac{g - E_t \epsilon}{b[\sigma - g]} \left| 1 - \frac{1}{E} \frac{d\sigma}{d\epsilon} \right| \tag{A.1}$$

which is obtained from (24) and where b is given by (22). The arguments B, C, D of ψ are the free constants in the assumed representation of

$$\psi = B + \frac{C}{f(x/D)} \tag{A.2}$$

where $f\left(\frac{x}{D}\right)$ is an increasing function. Examples of such functions are given in Table 2. Since $\psi[0] = \bar{E} = B + C/f[0]$ only two constants need

---

* $\bar{E} = \psi[0]$ is selected to be slightly less than E.

be determined in the subsequent nonlinear least square analysis* which employs (A.1), (A.2) and the fitted analytical expressions for σ and g (since the derivatives are needed in (A.1), analytical expressions are preferred). This analysis then yields the constants for (A.2).

With all the constants determined the model can now be integrated numerically and should reproduce the experimental results used to determine the constants. Due to the nonlinearity of the problem some iterations are probably necessary. These iterations may employ different forms of ψ and k consistent with the general requirements.

---

* The IMSL subroutine ZXSSQ is an example of possible algorithm

REFERENCES

1. S.R. Bodner and Y. Partom, "Constitutive Equations for Elastic-Viscoplastic Strain-Hardening Materials," Trans. ASME, J. Appl. Mech., 42, 385-389 (1975).

2. A.K. Miller, "An Inelastic Constitutive Model for Monotonic, Cyclic and Creep Deformation, Parts I and II," Trans. ASME, J. Eng. Matls. and Tech., 98, 97-113 (1976).

3. E.W. Hart, "Constitutive Relations for the Nonelastic Deformation of Metals," Trans. ASME, J. Eng. Matls. and Tech., 98, 193-201 (1976).

4. R.W. Rhode and J.C. Swearengen, "Deformation Modeling Applied to Stress Relaxation of Four Solder Alloys," Trans. ASME, J. Eng. Matls. and Tech., 102, 207-214 (1980).

5. J.L. Chaboche, "Viscoplastic Constitutive Equations for the Description of Cyclic and Anisotropic Behavior of Metals," Bull. de l'Acad. Polonaise des Sciences, Série Sc. et Techn., 25, 33-42 (1977).

6. K.P. Walker, "Research and Development Program for Nonlinear Structural Modeling with Advanced Time-Temperature Dependent Constitutive Relationships," NASA Report CR-165533, November 1981.

7. E.P. Cernocky and E. Krempl, "A Nonlinear Uniaxial Integral Constitutive Equation Incorporating Rate Effects, Creep, and Relaxation," Int'l. J. of Nonlinear Mechanics, 14, 183-203 (1979).

8. E. Krempl, "The Role of Servocontrolled Testing in the Development of the Theory of Viscoplasticity Based on Total Strain and Overstress," Amer. Society for Testing and Materials, STP 765, 5-28 (March 1982).

9. D. Kujawski and E. Krempl, "The Rate(Time)-Dependent Behavior of Ti-7Aℓ-2Cb-1Ta Titanium Alloy at Room Temperature under Quasi-Static Monotonic and Cyclic Loading," Trans. ASME, J. Appl. Mech., 48, 55-63 (1981).

10. E.P. Cernocky and E. Krempl, "A Coupled Theory of Thermoviscoplasticity Based on Total Strain and Overstress and its Predictions in Monotonic Torsional Loading," Journal of Thermal Stresses, 4, 69-82 (1981).

11. E.P. Cernocky and E. Krempl, "A Nonlinear Uniaxial Integral Constitutive Equation Incorporating Rate Effects, Creep, and Relaxation," Int'l. J. of Nonlinear Mechanics, 14, 183-203 (1979).

12. E. Krempl and V.V. Kallianpur, forthcoming.

13. E. Krempl and V.V. Kallianpur, "Some Critical Uniaxial Experiments for Viscoplasticity at Room Temperature," to appear J. Mech. Phys. Solids.

14. D. Kujawski, V.V. Kallianpur and E. Krempl, "An Experimental Study of Uniaxial Creep, Cyclic Creep and Relaxation of AISI Type 304 Stainless Steel at Room Temperature," J. Mechanics and Physics of Solids, 28, 129-148 (1980).

15. Y. Asada and S. Mitsuhashi, "Creep-Fatigue Interaction of Types 304 and 316 Stainless Steel in Air and Vacuum," Proc. 4th Int. Conf. on Pressure Vessel Technology, I. Mech. Eng., London, C48/80, 321-327, 1980.

16. J.J. McMahon, M.S. Thesis, Rensselaer Polytechnic Institute, Troy, New York, December 1983.

17. G. Wang, D. Yao and E. Krempl, "Viscoplasticity Based on Overstress with an Integral Growth Law for the Equilibrium Stress, RPI Report MML-83-2, October 1983; submitted for publication.

18. J.C. Swearengen and J.H. Holbrook, "Internal Variable Models for Rate-Dependent Plasticity: Analysis of Theory and Experiment," Sandia Report Sand. 83-8607, February 1984, to appear in Res. Mechanica.

19. E. Krempl, "An Experimental Study of Room-Temperature Rate Sensitivity, Creep and Relaxation of Type 304 Stainless Steel," J. Mechanics and Physics of Solids, 27, 363-375 (1979).

20. E. Krempl and H. Lu, "The Hardening and Rate-Dependent Behavior of Fully Annealed Type 304 Stainless Steel Under Biaxial In-Phase and Out-of-Phase Strain Cycling at Room Temperature," submitted to ASME 1984 WAM Symposium on Constitutive Equations. Micro and Macro Aspects.

21. H. Lu, forthcoming.

22. J.B. Conway, "An Analysis of the Relaxation Behavior of AISI 304 and 316 Stainless Steel at Elevated Temperatures," GEMP-730, General Electric Nuclear Systems Programs, Cincinnati, Ohio, December 1969.

23. E. Krempl, "Cyclic Creep. An Interpretive Literature Survey," WRC Bulletin No.195, Welding Research Council, New York, June 1974.

24. J.L. Chaboche, K. Dang Van and G. Cordier, "Modelization of the Strain Memory Effect on the Cyclic Hardening of 316 Stainless Steel," Paper L11/3, Proc. SmiRT V, Commission of the European Communities, 1979.

25. E. Krempl, "On the Interaction of Rate- and History-Dependence in Structural Metals," Acta Mechanica, 22, 53-90 (1975).

26. M.C.M. Liu and E. Krempl, "A Uniaxial Viscoplastic Model Based on Total Strain and Overstress," J. Mechanics and Physics of Solids, 27, 377-391 (1979).

27. M. Sutcu and E. Krempl, "Viscoplasticity Based on Overstress with a Differential Growth Law for the Equilibrium Stress," to be presented at 2nd Army Conference on Appl. Math. and Computing, May 1984, RPI, Troy, New York.

28. Unpublished Results, Mechanics of Materials Laboratory, Rensselaer Polytechnic Institute.

29. E.P. Cernocky and E. Krempl, "Construction of Nonlinear Monotonic Functions with Selectable Intervals of Almost Constant or Linear Behavior," Trans. ASME, J. Applied Mech., 45, 780-784 (1978).

30. J.L. Chaboche and G. Rousselier, "On Plastic and Viscoplastic Constitutive Equations - Part II: Application of Internal Variable Concepts to the 316 Stainless Steel," J. of Pressure Vessel Technology, 105, 159-164 (1983).

TABLE 1

SLOPES AFTER A JUMP IN STRESS OR STRAIN RATE

Change	Condition[1)]	$d\sigma^+/d\epsilon$		$dg^+/d\epsilon$	
		Strain Control	Stress Control	Strain Control	Stress Control
Increase	$0 < \delta \ll 1$	E	$\frac{E}{1+\delta E/E_t}$	ψ	$\frac{E\delta+\psi}{1+\delta E/E_t}$
Decrease	$\delta \gg 1$	$-\delta E$	E_t/δ	$\delta(E_t-\psi)$	E_t
Reversal	$\delta = -1$	$2E$	$-E_t$	$2\psi - E_t$	E_t
Reversal increase	$-1 \ll \delta < 0$	E	$\frac{E}{1+\delta E/E_t}$	ψ	$\frac{E\delta+\psi}{1+\delta E/E_t}$
Reversal decrease	$\delta \ll -1$	$-\delta E$	E_t/δ	$\delta(E_t-\psi)$	E_t

1) $\delta = \dot{\epsilon}^-/\dot{\epsilon}^+$ or $\dot{\sigma}^-/\dot{\sigma}^+$.

TABLE 2

MATERIAL CONSTANTS AND FUNCTIONS USED

E = Modulus of elasticity = 120,000 MPa

E_t = Asymptotic tangent modulus = 1200 MPa

A = 120 MPa

† $k[x] = 2.296 \times 10^{-4} \exp\left(21.275 \exp - \frac{|x|}{58.28}\right)$ s

$\psi_1[x] = 48{,}000 + 70{,}800 \exp(-0.12\ |x|)$ MPa

Used in all figures except in Figures 6 and 8

$\psi_2[x] = 12{,}000 + 106{,}800 \cosh(-0.2\ |x|)$ MPa

Used in Figures 6 and 8

† All x used here are measured in units of MPa.

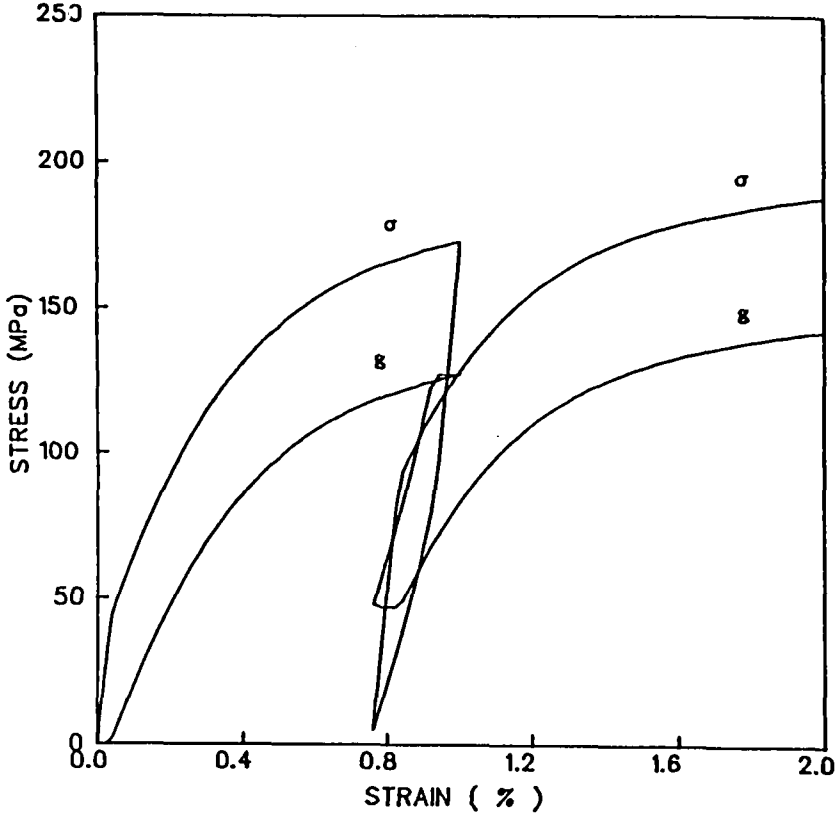

Figure 1 The Evolution of σ and g During Loading, Unloading and Reloading Under Strain Control. The function ψ_1 is multiplied by $\dot{\varepsilon}^{in}$. Material functions used are given in Table 2. $|\dot{\varepsilon}| = 10^{-4}\ s^{-1}$.

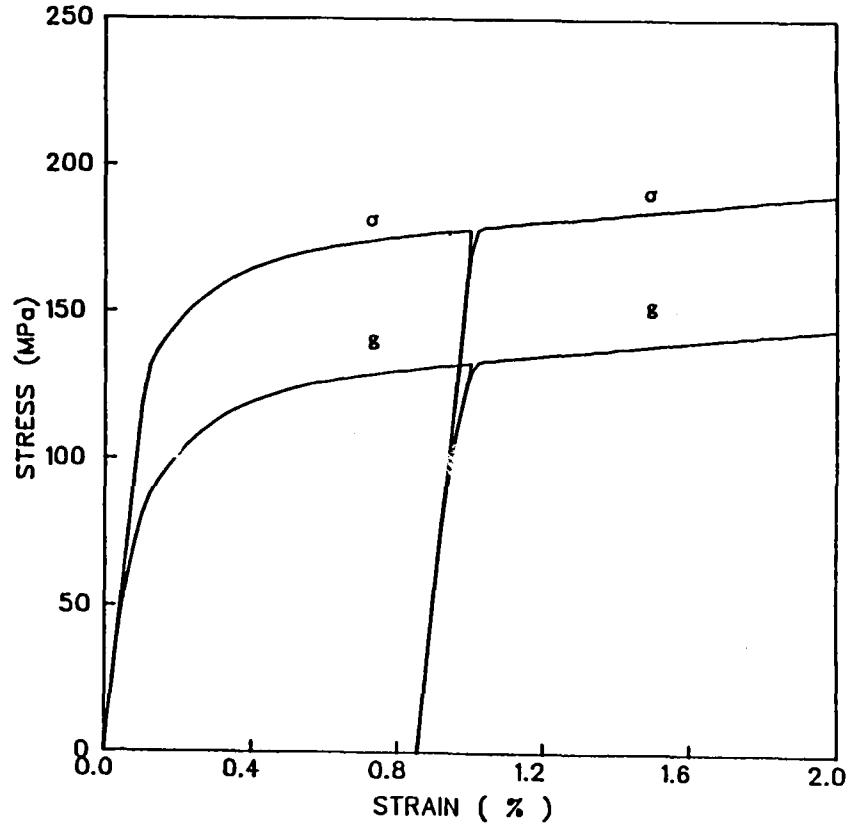

Figure 2 Same as Figure 1 Except that ψ_1 is Multiplied by $\dot{\varepsilon}$. Regions of almost linear elastic behavior are those where σ = g.

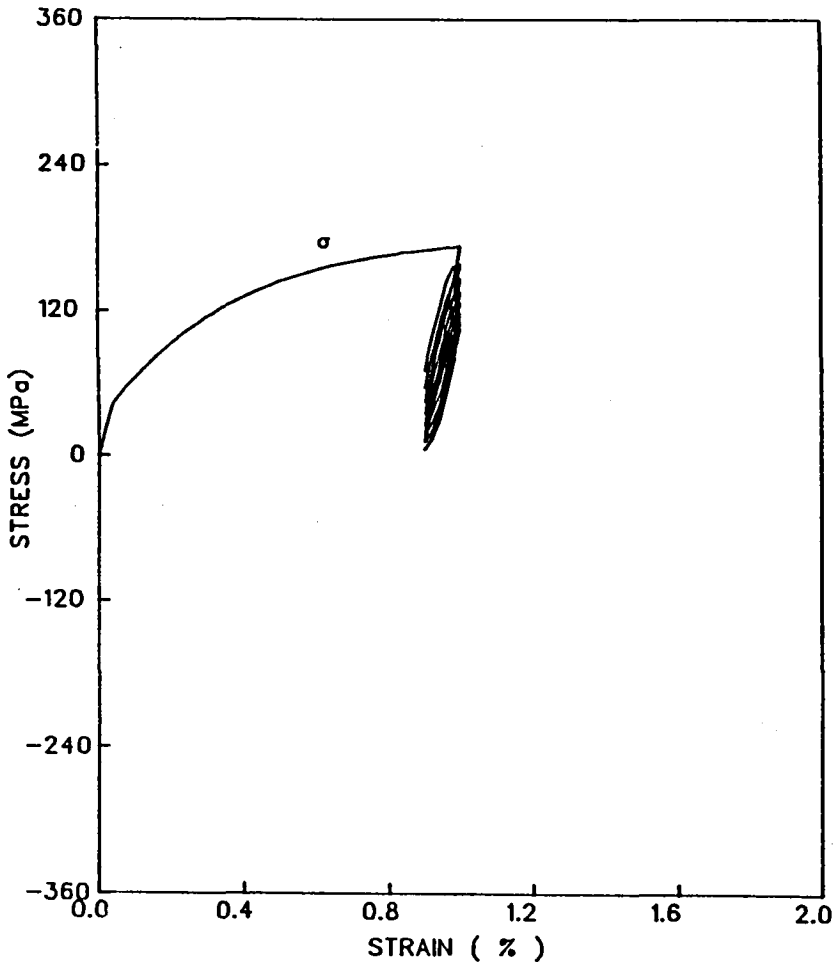

Figure 3 Strain Controlled Loading with Positive Mean Strain. $\epsilon_{max} = 1.0\%$, $\epsilon_{min} = 0.9\%$, $|\dot{\epsilon}| = 10^{-4}\ s^{-1}$. The function ψ_1 is multiplied by $\dot{\epsilon}^{in}$. Material functions are given in Table 2. The equilibrium curve g is not plotted.

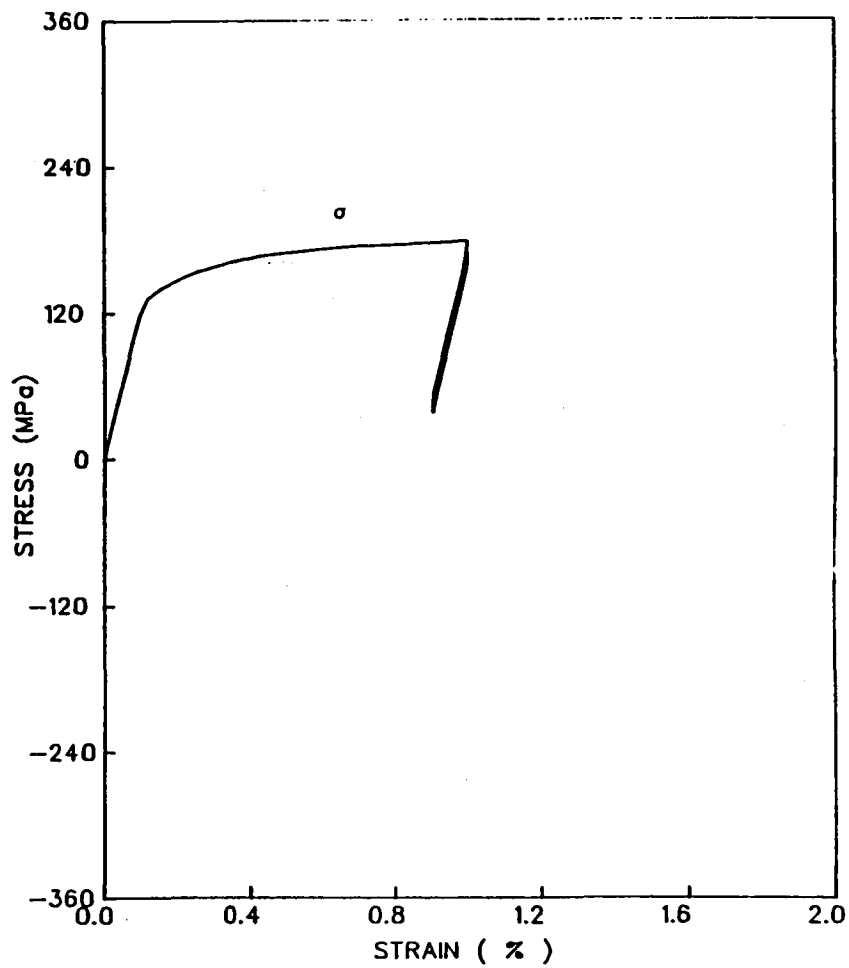

Figure 4 Same as Figure 3 Except that ψ_1 is Multiplied by $\dot{\epsilon}$

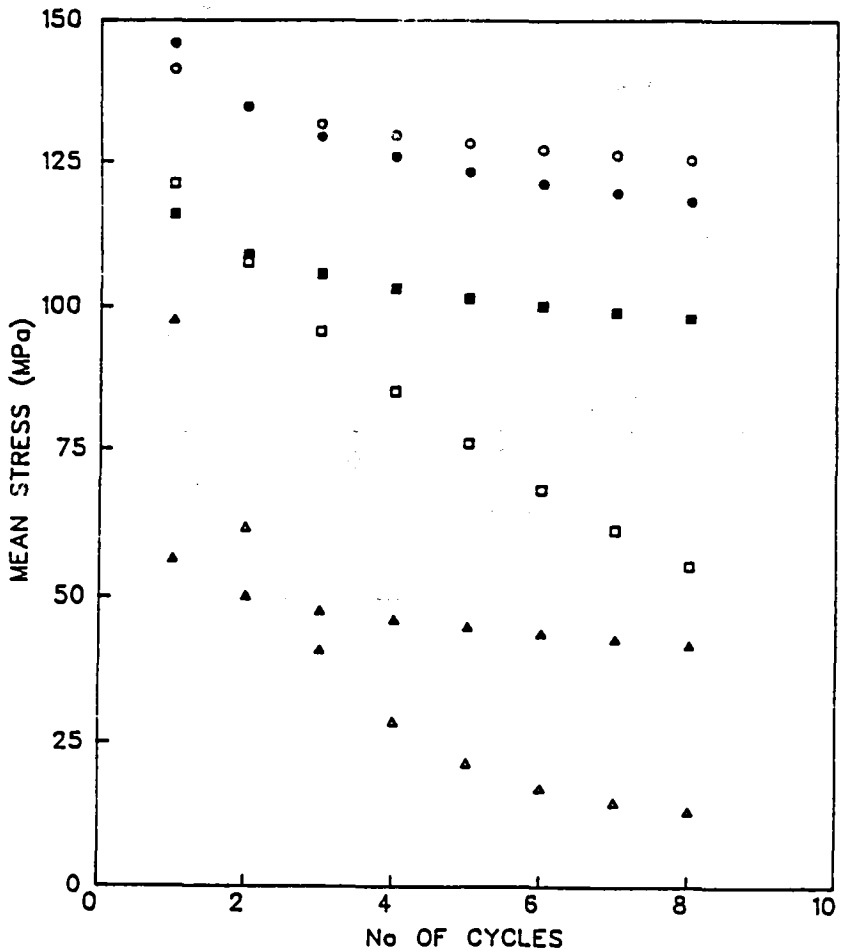

Figure 5 Evolution of Mean Stress with Cycles for the Conditions of Figures 3 and 4. Open symbols $\dot{\epsilon}^{in}$ multiplies ψ_1. Filled symbols $\dot{\epsilon}$ multiplies ψ_1.

○ $\epsilon_{max} = 1.0\%$ $\epsilon_{min} = 0.9\%$ $|\dot{\epsilon}| = 10^{-2}\ s^{-1}$

□ $\epsilon_{max} = 1.0\%$ $\epsilon_{min} = 0.9\%$ $|\dot{\epsilon}| = 10^{-4}\ s^{-1}$

Δ $\epsilon_{max} = 1.0\%$ $\epsilon_{min} = 0.8\%$ $|\dot{\epsilon}| = 10^{-4}\ s^{-1}$

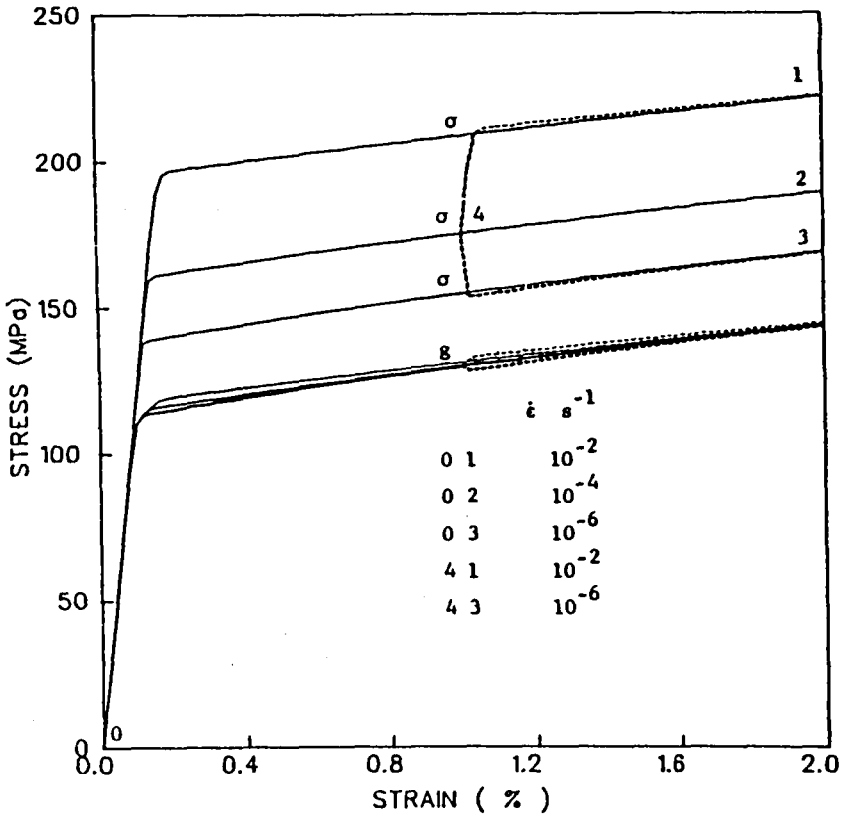

Figure 6 Evolution of σ and g During Constant Strain Rate Loading and During Sudden Changes in Strain Rate. The function ψ_2 of Table 2 is used.

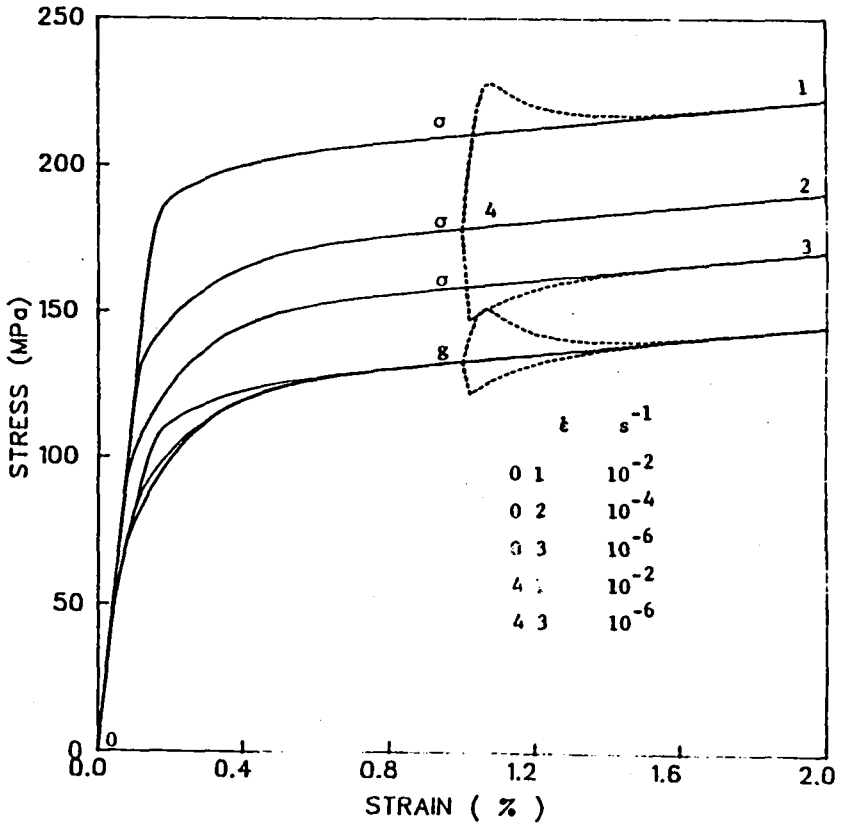

Figure 7 Same as Figure 6 Except that ψ_1 of Table 2 is Used

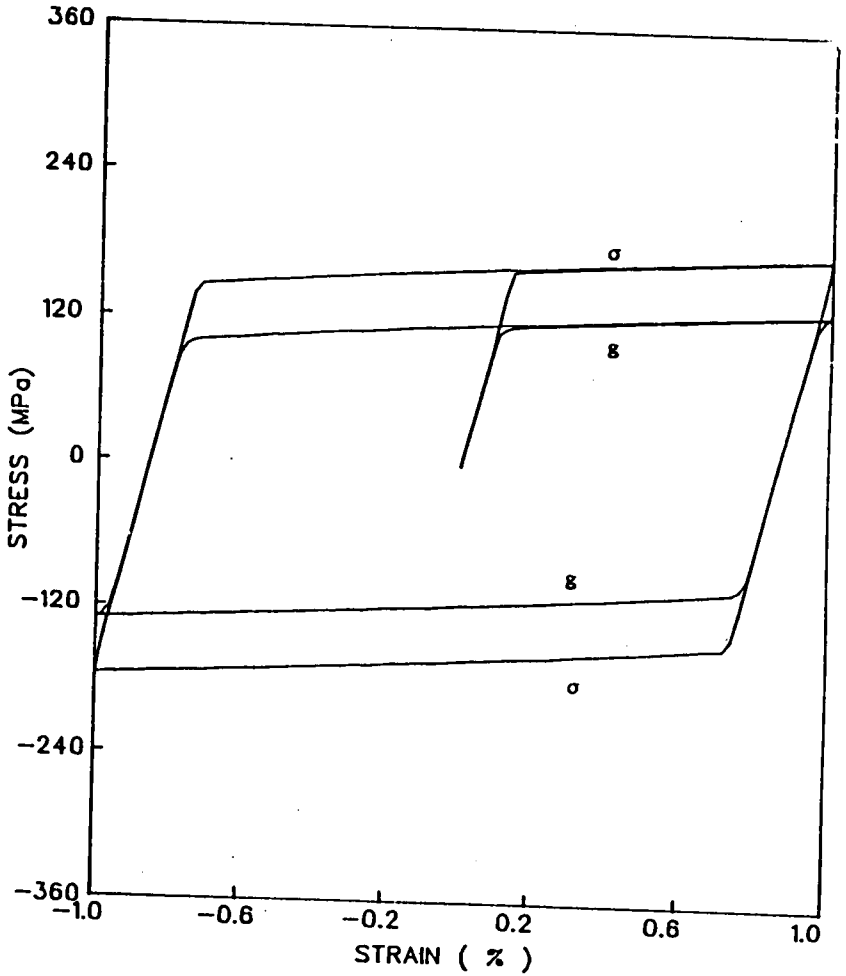

Figure 8 One Hysteresis Loop Represented by the Functions Used in Figure 6

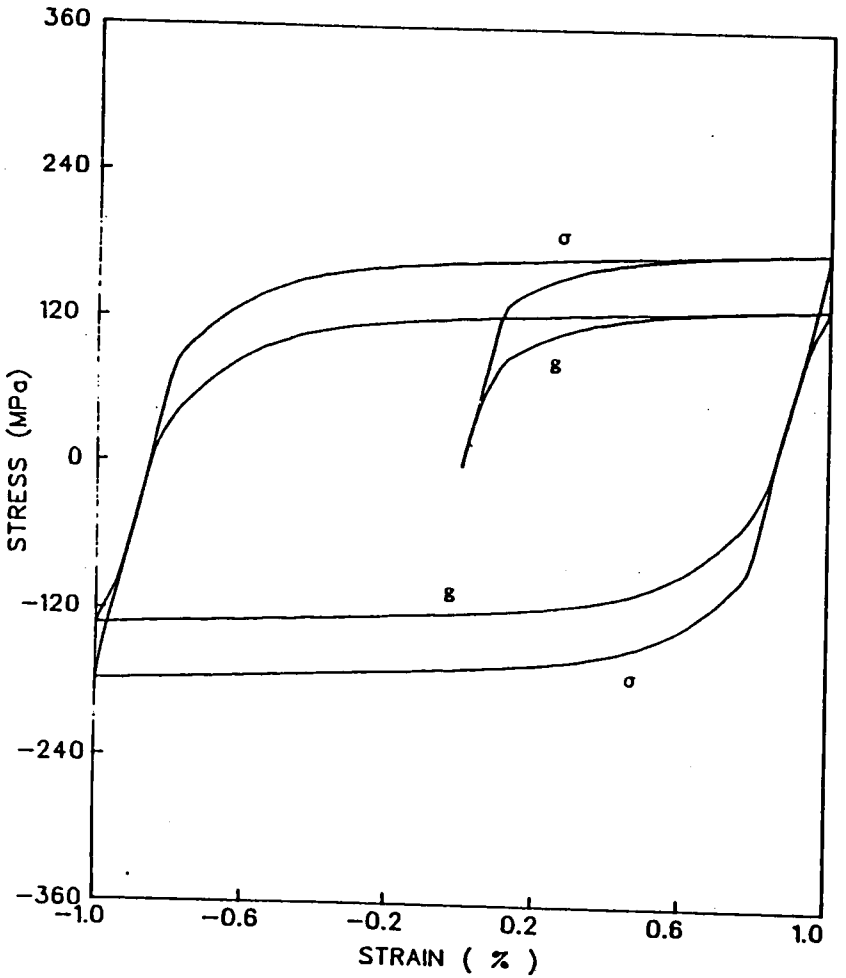

Figure 9 One Hysteresis Loop Represented by the Functions Used in Figure 7

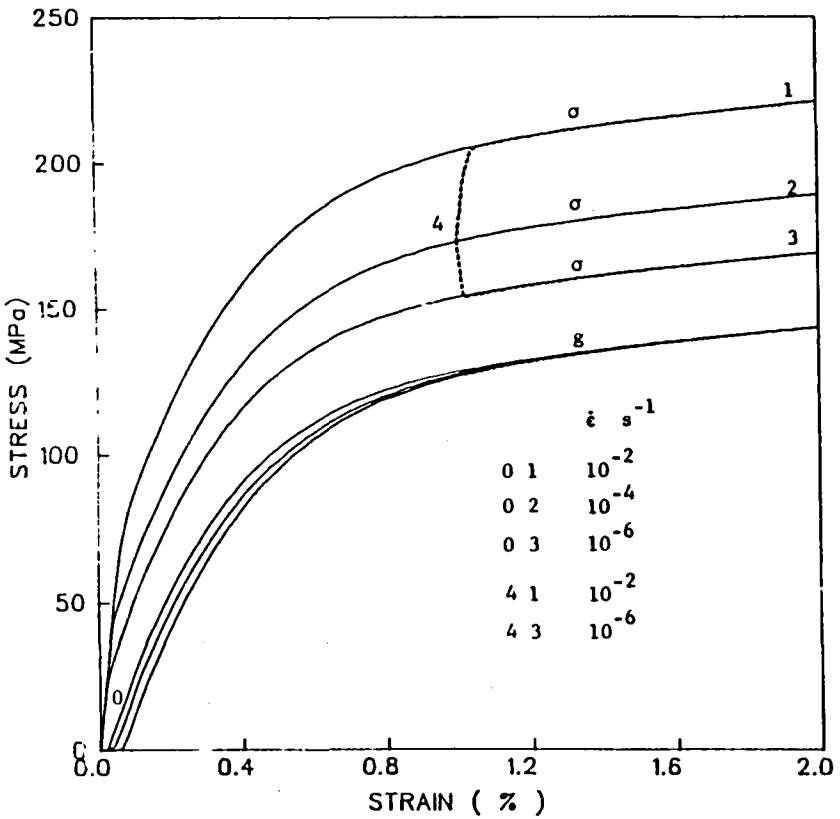

Figure 10 Same as Figure 7 Except $\dot{\epsilon}^{in}$ is Used to Multiply ψ_1

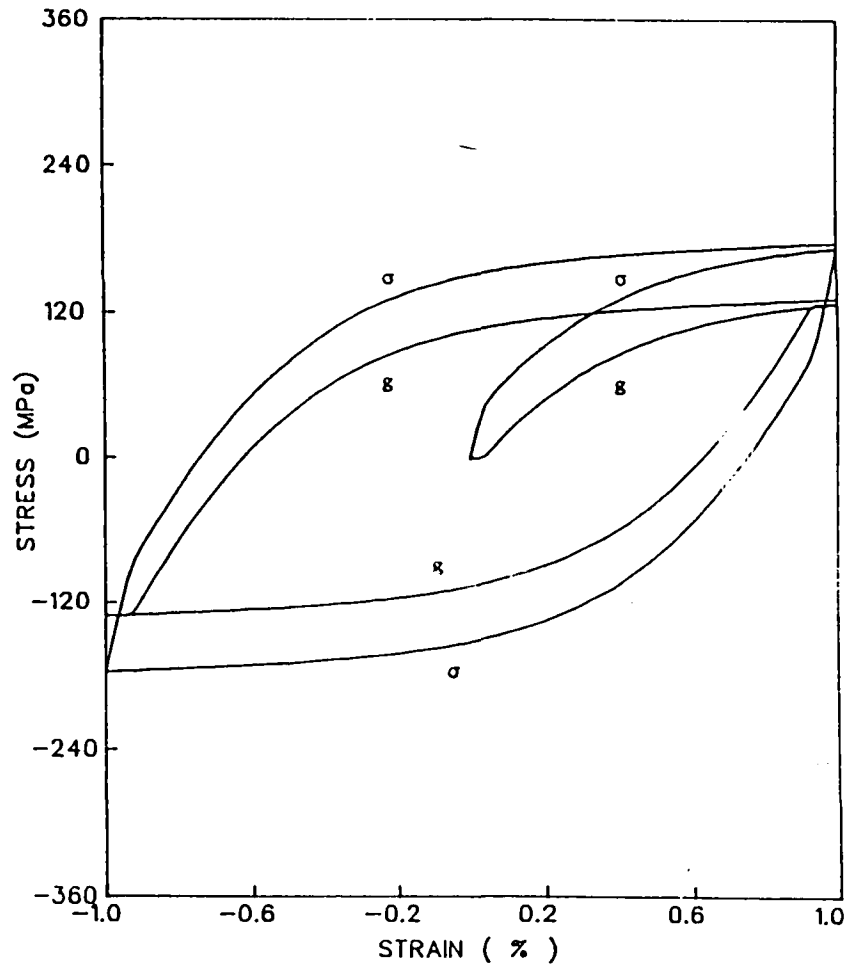

Figure 11 Same as Figure 9 Except that $\dot{\epsilon}^{in}$ is Used to Multiply ψ_1